

Chelate ring-opening aminophosphine complexes of ruthenium(II)

Robert Morris, Abraha Habtemariam, Zijian Guo, Simon Parsons, Peter J. Sadler*

School of Chemistry, The University of Edinburgh, King's Building, West Mains Road, Edinburgh EH9 3JJ, UK

Received 22 February 2002; accepted 17 May 2002

Dedicated in honor of Professor Helmut Sigel

Abstract

The preparations and X-ray crystal structures of the Ru(II) aminophosphine complexes *trans*, *cis*-[RuCl₂(H(Bz)NCH₂CH₂PPh₂-*N,P*)₂] (**1**), *trans*, *cis*-[RuCl₂(H₂NCH₂CH₂PPh₂-*N,P*)₂] (**3**) and [(η⁶-C₆H₆)Ru(PPh₂CH₂CH₂NMe₂-*N,P*)Cl][PF₆] (**5**) are described. Complexes **1** and **3** are octahedral and contain a marked distortion of the Cl–Ru–Cl axis from linearity. Complex **3** undergoes facile chelate ring-opening in DMSO and CH₃CN solutions to give complexes containing one chelated aminophosphine ligand and one pendant ligand coordinated only through P. The X-ray structure of *trans*, *cis*-[RuCl₂(DMSO-*S*)₂(H₂NCH₂CH₂P(O)Ph₂-*N,O*)] (**4**) containing an oxidised aminophosphine ligand is also reported.

© 2002 Elsevier Science B.V. All rights reserved.

Keywords: Ruthenium(II); Aminophosphine ligands; X-ray structures; Chelate ring-opening

1. Introduction

There are many previous reports of the potential use of aminophosphine complexes, mainly in relation to catalysis [1]. However, very few studies [2] have investigated the biological activity of such complexes even though they contain *cis* amine ligands, a feature found in many active platinum anti-cancer agents [3]. Chelate ring-opened aminophosphine complexes also possess lipophilic-cationic character and have the potential to exhibit cytotoxicity by disrupting mitochondrial function [4]. Octahedral d⁶ Ru(II) centres can provide more reaction sites than square-planar d⁸ Pt(II) and Pd(II) and in addition, nitrogen ligands would be expected to bind more weakly than phosphorus, thus offering the possibility of activation via chelate ring-opening [5,6].

Although some Ru–aminophosphine complexes have been synthesised previously [7,8], only a few X-ray crystal structures have been reported. These include the five coordinate complex dichloro(*o*-diphenylphosphino-*N,N*-dimethylaniline)-[tris(*p*-tolyl)phosphine]-

ruthenium(II) [7], *trans*-dichloro-*N,N'*-bis[(*o*-(di-phenylphosphino)benzylidene)ethylenediamine-ruthenium(II) where the aminophosphine ligand is tetradentate [9], and the dimeric structure of [Ru₂Cl₂(P–N)₄]²⁺, where P–N is 1-(diphenyl-phosphino)-2-(2-pyridyl)ethane [10]. We have previously reported [11] the synthesis and characterisation of the Ru(II) complex *trans*, *cis*-[RuCl₂(Me₂NCH₂CH₂PPh₂-*P,N*)₂]. This complex underwent a two step reaction in methanol involving chloride dissociation followed by P–N chelate ring-opening.

In this paper, we report the synthesis and crystal structures of Ru(II) aminophosphine complexes of the ligands shown in Fig. 1. We have studied chelate ring-opening reactions and considered possible biological applications.

2. Experimental

2.1. Chemicals

The following were used as received: RuCl₃·3H₂O (Johnson Matthey), 1,4-cyclohexadiene (Acros). Acetonitrile used for cyclic voltammetric studies was pre-dried with K₂CO₃ followed by distillation from CaH₂.

* Corresponding author. Tel.: +44-131-650 4729; fax: +44-131-650 6452

E-mail address: p.j.sadler@ed.ac.uk (P.J. Sadler).

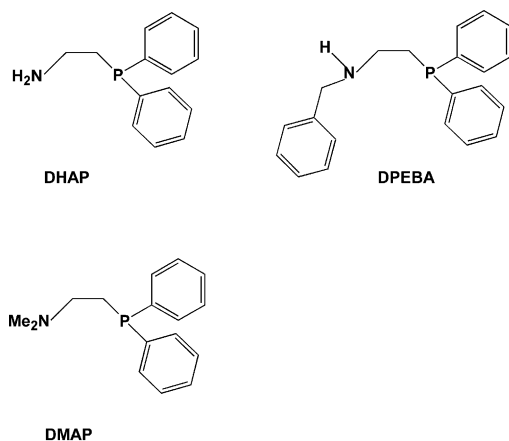


Fig. 1. Structures of the ligands used. Abbreviations: DHAP, 1-amino-2-diphenylphosphinoethane; DMAP, 1-dimethylamino-2-diphenylphosphinoethane; DPEBA, 1-benzylamino-2-diphenylphosphinoethane.

2.2. Measurements

Ultraviolet and visible spectra were obtained on a Perkin–Elmer Lambda 16 UV–Vis recording spectrophotometer using 1 cm path length quartz cuvettes. The temperature was controlled using a PTP1 Peltier Temperature Programmer. Spectra were normally referenced to solvent alone. Spectra were processed with UVWIN-LAB for WINDOWS '95.

^1H and $^{31}\text{P}\{^1\text{H}\}$ NMR spectra were recorded at 298 K on Bruker DMX500 (^1H 500 MHz; ^{31}P 202 MHz) and Varian-Inova 600 spectrometers (^1H 600 MHz), using 5 mm NMR tubes. The chemical shift references were as follows: ^1H (internal, TSP), ^{31}P (external, 30% H_3PO_4). The 2D gradient-selected $^1\text{H}, ^1\text{H}$ -COSY and TOCSY (mixing time of 0.12 s) experiments were carried out using standard sequences. Data sets with 2048×512 points were acquired with frequency widths of 8000 Hz in both dimensions and 16 scans per t_1 increment. The t_1 dimension was zero-filled to 2048 data points, and the spectrum was processed with a combination of exponential and Gaussian weighting functions. The 2D [$^1\text{H}, ^{31}\text{P}$] HSQC NMR spectra were recorded using a standard sequence. The ^{31}P -spins were decoupled by irradiation with the GARP-1 sequence during acquisition.

Cyclic voltammetry experiments were carried out in CH_3CN –[$n\text{-Bu}_4\text{N}][\text{BF}_4]$ (0.4 M), with an Autolab PGSTAT20 potentiostat equipped with GPES 4.2 software. The working electrode was a platinum microdisc of diameter 0.5 mm and the potential reported is quoted relative to a Ag/AgCl reference electrode via $\text{FeCp}_2\text{--FeCp}_2^+$ (0.375 V).

2.3. Preparation of ligands and starting complexes

The following were synthesised according to published procedures: $\text{H}_2\text{NCH}_2\text{CH}_2\text{PPh}_2$ (DHAP),

$\text{Me}_2\text{NCH}_2\text{CH}_2\text{PPh}_2$ (DMAP), $\text{H}(\text{Bz})\text{NCH}_2\text{CH}_2\text{PPh}_2 \cdot 2\text{HCl}$ (DPEBA) [5] and the complexes *cis*- and *trans*- $[\text{RuCl}_2(\text{DMSO})_4]$ [12], $[(\text{COD})\text{RuCl}_2]_x$ [13], and $[(\eta^6\text{-C}_6\text{H}_6)\text{Ru}(\text{CH}_3\text{CN})_2\text{Cl}][\text{PF}_6]$ [14].

2.4. Preparation of complexes

2.4.1. Synthesis of *trans*, *cis*- $[\text{RuCl}_2(\text{H}(\text{Bz})\text{NCH}_2\text{CH}_2\text{PPh}_2\text{-N,P})_2]$ (1)

cis- $[\text{RuCl}_2(\text{DMSO})_4]$ (0.24 g, 0.5 mmol) was stirred in acetone (10 ml) and the ligand DPEBA (0.36 g, 1 mmol) added in one portion. This was sealed and the reaction stirred overnight at ambient temperature. Ether was added to induce precipitation of a pink solid, which was collected and recrystallised from acetone–ether.

Yield: 4 mg, 1%. Calc. for $\text{C}_{42}\text{H}_{44}\text{Cl}_2\text{N}_2\text{P}_2\text{Ru}$: C, 62.22; H, 5.47; N, 3.46. Found: C, 61.63; H, 5.80; N, 3.71%. Single crystals of complex 1 suitable for X-ray analysis were grown from an acetone–ether mixture.

2.4.2. Synthesis of *trans*, *cis*- $[\text{RuCl}_2(\text{Me}_2\text{NCH}_2\text{CH}_2\text{PPh}_2\text{-N,P})_2]$ (2)

The ligand DMAP (0.36 g, 1.4 mmol) dissolved in benzene (5 ml) was added to a stirred suspension of $[\text{Ru}(\text{COD})\text{Cl}_2]_x$ (0.39 g, 1.4 mmol) in benzene (10 ml). The reaction was refluxed for 24 h and filtered while hot to remove unreacted ruthenium starting material. The red filtrate was evaporated to dryness and recrystallised from toluene.

Yield: 0.33 g, 34.6%. Calc. for $\text{C}_{32}\text{H}_{40}\text{Cl}_2\text{N}_2\text{P}_2\text{Ru}$: C, 55.98; H, 5.87; N, 4.08. Found: C, 55.53; H, 5.63; N, 3.92%. $^{31}\text{P}\{^1\text{H}\}$ NMR (d^8 -toluene): δ 57.0.

2.4.3. Synthesis of *trans*, *cis*- $[\text{RuCl}_2(\text{H}_2\text{NCH}_2\text{CH}_2\text{PPh}_2\text{-N,P})_2]$ (3)

The ligand DHAP (1.15 g, 5 mmol) was added in one portion to a stirred suspension of $[\text{Ru}(\text{COD})\text{Cl}_2]_x$ (0.7 g, 2.5 mmol) in benzene (40 ml) and the mixture refluxed under argon. After 4 h, a yellow precipitate had formed. This was collected after cooling and recrystallised from CH_2Cl_2 –ether.

Yield: 0.20 g, 12.8%. Calc. for $\text{C}_{28}\text{H}_{32}\text{Cl}_2\text{N}_2\text{P}_2\text{Ru}$: C, 53.34; H, 5.12; N, 4.44. Found: C, 53.95; H, 5.16; N, 3.07%. $^{31}\text{P}\{^1\text{H}\}$ NMR (d^6 -DMSO): δ 60.7 (d, $J = 24.6$ Hz), 45.7 (d, $J = 24.6$ Hz). Crystals of complex 3 suitable for X-ray analysis were grown by the slow evaporation of an ethanolic solution.

2.4.4. Synthesis of *trans*, *cis*- $[\text{RuCl}_2(\text{DMSO-S})_2(\text{H}_2\text{NCH}_2\text{CH}_2\text{P}(\text{O})\text{Ph}_2\text{-N,O})]$ (4)

trans- $[\text{RuCl}_2(\text{DMSO})_4]$ (0.06 g, 0.13 mmol) was set stirring in freshly dried ethanol (10 ml). DHAP (0.03 g, 0.13 mmol) was added in one portion and the yellow solution stirred overnight. An orange precipitate formed

during this time. This was collected and recrystallised from ethanol–ether.

Yield: 6 mg, 7.3%. $^{31}\text{P}\{^1\text{H}\}$ NMR (CDCl_3): δ 51.6 (s). Complex **4** was obtained as single crystals suitable for X-ray analysis by diffusion of ether into an ethanol solution.

2.4.5. Synthesis of $[(\eta^6\text{-C}_6\text{H}_6)\text{Ru}(\text{Me}_2\text{NCH}_2\text{CH}_2\text{PPh}_2\text{-N,P})\text{Cl}][\text{PF}_6]$ (**5**)

DMAP (0.077 g, 0.23 mmol) dissolved in dry acetonitrile (2 ml) was added in one portion to a solution of $[(\eta^6\text{-C}_6\text{H}_6)\text{Ru}(\text{CH}_3\text{CN})_2\text{Cl}][\text{PF}_6]$ (0.102 g, 0.23 mmol) in dry acetonitrile (8 ml). The mixture was stirred at ambient temperature for 10 h in a sealed flask with no special precautions to exclude air. The orange solution was evaporated to an orange oil which was taken up in 2 ml CHCl_3 . Ether was added to induce precipitation and the orange solid was collected, washed with ether and recrystallised as the 0.5 CH_3CN solvate by slow diffusion of ether into an acetonitrile solution.

Yield: 0.085 g, 57.8%. Calc. for $\text{C}_{23}\text{H}_{27.5}\text{Cl-F}_6\text{N}_{1.5}\text{P}_2\text{Ru}$: C, 43.30; H, 4.35; N, 3.29. Found: C, 43.05; H, 4.40; N, 3.03%. ^1H NMR (CD_3CN): δ 5.68 (d, 6H), 3.19 (s, 3H), 3.11 (s, 3H). $^{31}\text{P}\{^1\text{H}\}$ NMR (CD_3CN): δ 57.9 (s). Crystals of complex **5** suitable for X-ray analysis were grown by diffusion of ether into an acetonitrile solution.

2.5. X-ray crystallographic analysis

Data for **1**, **4** and **5** were collected on Stoe Stadi-4 diffractometers using conventional sealed-tube sources, the data set for **3** was collected using synchrotron radiation with a Bruker SMART diffractometer on Station 9.8 at the Synchrotron Radiation Source at Daresbury, UK. Both instruments were equipped with Oxford Cryosystems low-temperature devices. The structures were solved by Patterson methods (DIRDIF or SHELXTL) [15,16] and refined by full-matrix least-squares against F^2 (SHELXTL). In all cases H-atoms were placed in calculated positions.

2.5.1. Crystal data for **1**

$\text{C}_{42}\text{H}_{44}\text{Cl}_2\text{N}_2\text{P}_2\text{Ru}$, $M = 810.70$, triclinic, space group $P\bar{1}$, $a = 10.920(6)$, $b = 12.061(7)$, $c = 16.696(9)$ Å, $\alpha = 97.35(5)^\circ$, $\beta = 106.74(5)^\circ$, $\gamma = 111.50(4)^\circ$, $V = 1890.8(18)$ Å³, $T = 220$ K, $Z = 2$, $\rho_{\text{calc}} = 1.424$ mg m⁻³. Orange block $0.19 \times 0.16 \times 0.12$ mm. The crystal was rather weakly diffracting, and so data were collected with Cu K α radiation; an absorption correction was applied using ψ -scan data ($\mu = 5.700$ mm⁻¹, range of transmission: 0.474–0.704) [16]. One carbon atom (labelled C3 in the tables) is disordered over two positions; similarity restraints were applied to the geometries of the two part-weight components. $R_1 = 7.64\%$ (based on F and 2833 data with $F > 4\sigma(F)$) and $wR_2 = 17.56\%$ (based on F^2

and all 5534 unique data to $2\theta = 120^\circ$). The final difference map extremes were $+0.70$ and -0.81 e Å⁻³.

2.5.2. Crystal data for **3**

$\text{C}_{28}\text{H}_{32}\text{Cl}_2\text{N}_2\text{P}_2\text{Ru}$, $M = 630.47$, triclinic, space group $P\bar{1}$, $a = 9.9837(8)$, $b = 10.4950(9)$, $c = 15.2046(13)$ Å, $\alpha = 77.502(2)^\circ$, $\beta = 75.694(2)^\circ$, $\gamma = 63.886(2)^\circ$, $V = 1375.5(2)$ Å³, $T = 150$ K, $Z = 2$, $\rho_{\text{calc}} = 1.522$ mg m⁻³. Orange block $0.20 \times 0.06 \times 0.06$ mm. The crystal was rather weakly diffracting, and so data were collected using synchrotron radiation ($\lambda = 0.6878$ Å); an absorption correction was applied using Sadabs [17] ($\mu = 0.901$ mm⁻¹, range of transmission: 0.449–0.928) [18]. $R_1 = 3.78\%$ (based on F and 6496 data with $F > 4\sigma(F)$) and $wR_2 = 9.55\%$ (based on F^2 and all 7321 unique data to $2\theta = 59^\circ$). The final difference map extremes were $+1.63$ and -0.93 e Å⁻³. Dispersion terms were calculated using FPRIME [18].

2.5.3. Crystal data for **4**

$\text{C}_{18}\text{H}_{28}\text{Cl}_2\text{NO}_3\text{PRuS}_2$, $M = 573.47$, monoclinic, $P2_1/c$, $a = 11.459(9)$, $b = 11.938(8)$, $c = 17.886(16)$ Å, $\beta = 106.63(6)^\circ$, $V = 2344.4(8)$ Å³, $T = 220$ K, $Z = 4$, $\rho_{\text{calc}} = 1.625$ mg m⁻³. Orange block, $0.45 \times 0.27 \times 0.19$ mm, Mo K α radiation $\mu = 1.162$ mm⁻¹. The peak profiles were rather asymmetric and misshapen, and possibly for this reason an attempt to perform an absorption correction based on ψ -scan measurements was unsuccessful; a correction using SHELXA [16] was applied after isotropic refinement (range of transmission: 0.05–0.46). Only the Ru, Cl, P, S and O atoms were refined anisotropically. $R_1 = 12.0\%$ (based on F and 1370 data with $F > 4\sigma(F)$) and $wR_2 = 35.710\%$ (based on F^2 and all 3061 unique data to $2\theta = 45^\circ$). The final difference map extremes were $+1.25$ and -1.67 e Å⁻³. Clearly this is a low-precision determination, and the results were only used to establish chemical connectivity.

2.5.4. Crystal data for **5**

$\text{C}_{23}\text{H}_{27.5}\text{ClF}_6\text{N}_{1.5}\text{P}_2\text{Ru}$, $M = 637.43$, monoclinic, $P2_1/c$, $a = 10.954(3)$, $b = 16.076(5)$, $c = 15.159(4)$ Å, $\beta = 110.45(2)^\circ$, $V = 2501.2(12)$ Å³, $T = 150$ K, $Z = 4$, $\rho_{\text{calc}} = 1.693$ mg m⁻³. Orange block, $0.45 \times 0.45 \times 0.45$ mm, Mo K α radiation $\mu = 0.921$ mm⁻¹. An absorption correction was applied using ψ -scan data (range of transmission: 0.478–0.548). One phenyl group and the PF_6^- anion are disordered over two orientations; the acetonitrile of solvation is disordered about a crystallographic inversion centre. $R_1 = 3.69\%$ (based on F and 4092 data with $F > 4\sigma(F)$) and $wR_2 = 9.27\%$ (based on F^2 and all 4414 unique data to $2\theta = 50^\circ$). The final difference map extremes were $+0.86$ and -0.65 e Å⁻³.

3. Results and discussion

3.1. Preparation and properties of ligands

The ligands, prepared by literature methods [5], were obtained as viscous oils (DMAP and DHAP) or as a hydrochloride salt (DPEBA). The oily ligands were readily purified by passing ether solutions through a short column of alumina or by reduced-pressure distillation. The DPEBA ligand was recrystallised from methanol–ether.

The mixed donor ligands DMAP, DHAP and DPEBA are soluble in almost all organic solvents. The ^1H NMR spectra of the ligands in CDCl_3 showed the expected peaks with the backbone $-\text{CH}_2-$ giving multiplets and the $-\text{NH}_2$ a broad peak at δ 1.5 (DHAP). The $^{31}\text{P}\{^1\text{H}\}$ NMR spectra showed singlet resonances in the region of -19 to -22 ppm.

3.2. Preparation and properties of ruthenium(II) complexes

$\text{cis-}[\text{RuCl}_2(\text{DMSO})_4]$ is a very versatile reagent known to provide a very good entry point to Ru(II) chemistry. A large number of Ru(II) complexes have been synthesised from it [19], including the chelate-ring opening aminophosphine complex $[\text{RuCl}_2(\text{DMAP})_2]$ [11]. The easily displaced DMSO ligands make possible the formation of Ru(II) chloride complexes with a variety of ligands.

The reaction of $\text{cis-}[\text{RuCl}_2(\text{DMSO})_4]$ with DPEBA as its hydrochloride salt in a 1:2 molar ratio, in acetone, gave rise to $\text{trans, cis-}[\text{RuCl}_2(\text{H}(\text{Bz})\text{NCH}_2\text{CH}_2\text{PPh}_2\text{-}N,P)_2]$ (**1**). Attempts to prepare **1** in CH_2Cl_2 resulted in an air-sensitive, uncharacterisable reddish solid.

The 1:1 reaction of the ligand DMAP and $[\text{Ru}(\text{COD})\text{Cl}_2]_x$ in refluxing benzene produced the complex $\text{trans, cis-}[\text{RuCl}_2(\text{Me}_2\text{NCH}_2\text{CH}_2\text{PPh}_2\text{-}N,P)_2]$ (**2**). It was hoped that this product would contain one coordinated ligand and an η^4 -coordinated cyclooctadiene. However, under the conditions used, the COD ligand proved to be too labile and was displaced by two aminophosphine ligands. Complex **2** is a known complex [11,20].

The reaction of $[\text{Ru}(\text{COD})\text{Cl}_2]_x$ with DHAP in refluxing benzene in a 1:2 molar ratio resulted in the displacement of the COD ligand and the coordination of two DHAP ligands to form $\text{trans, cis-}[\text{RuCl}_2(\text{H}_2\text{NCH}_2\text{CH}_2\text{PPh}_2\text{-}N,P)_2]$ (**3**). The complex was characterised by elemental analysis and X-ray crystallography. Complex **3** is reasonably soluble only in coordinating solvents such as DMSO and acetonitrile, and sparingly soluble in alcohols.

One batch of our aminophosphine ligand DHAP contained both reduced (^{31}P δ -21.0) and oxidised ($\text{P}=\text{O}$ δ 32.6 , c.f. $\text{Ph}_3\text{P}=\text{O}$ δ 31.0 [21]) forms of the

ligand in a 4:1 ratio. When this was reacted with $\text{trans-}[\text{RuCl}_2(\text{DMSO})_4]$ in a 1:1 molar ratio we obtained the aminophosphine oxide complex $\text{trans, cis-}[\text{RuCl}_2(\text{DMSO-}S)_2(\text{H}_2\text{NCH}_2\text{CH}_2\text{P}(\text{O})\text{Ph}_2\text{-}N,O)]$ (**4**), in very low yield. Ruthenium phosphine oxide complexes can be difficult to isolate due to the lability of the phosphine oxide ligands in solution [22], for example a Ru(II)terpy complex with $(\text{O})\text{Ph}_2\text{PCH}_2\text{CH}_2\text{PPh}_2(\text{O})$ has been reported to dissociate rapidly in solution [21]. The ^{31}P NMR spectrum of complex **4** in CDCl_3 showed a singlet at 51.6 ppm.

The reaction of $[(\eta^6\text{-C}_6\text{H}_6)\text{Ru}(\text{CH}_3\text{CN})_2\text{Cl}][\text{PF}_6]$ with DMAP in acetonitrile followed by work-up produced red crystals of the complex $[(\eta^6\text{-C}_6\text{H}_6)\text{Ru}(\text{DMAP-}N,P)\text{Cl}][\text{PF}_6]$ (**5**) in moderate yield. Complex **5** is soluble in alcohols and coordinating solvents such as DMSO and acetonitrile, but insoluble in water or mixed solvents containing an appreciable amount ($>20\%$) of water. The ^1H NMR spectrum in CD_3CN shows a doublet for the π -coordinated benzene ring due to coupling with ^{31}P , implying that all the protons on the benzene ring are equivalent and hence there is free rotation of the π -coordinated benzene ligand. The NMe_2 groups of the chelated ligand gave rise to two singlets at δ 3.11 and 3.19, indicating that the two methyl groups are nonequivalent, as expected since the Ru(II) centre is chiral. The ^{31}P NMR spectrum showed a singlet at δ 58, appropriate for a ring-closed structure. The $^{13}\text{C}\{^1\text{H}\}$ NMR spectrum contained resonances at δ 125–135 for the P-Ph_2 carbons, and a doublet at δ 89.3 for the η^6 -coordinated benzene ring, due to coupling to ^{31}P , ($J_{\text{CP}} = 2.95$ Hz). The N-CH_2- signal appeared as doublet at δ 60.5 ($J_{\text{CP}} = 2.98$ Hz), and the P-CH_2- resonance as doublet at δ 25.6 ($J_{\text{CP}} = 26.66$ Hz). The two N-CH_3 signals were singlets at δ 58.3 and 56.5. There was no change in the NMR spectrum after 3 days incubation at 300 K, showing that chelate-ring opening does not occur in CD_3CN , a coordinating solvent.

3.3. NMR analysis of chelate ring-opening of complex 3

Complex **3** $\text{trans, cis-}[\text{RuCl}_2(\text{H}_2\text{NCH}_2\text{CH}_2\text{PPh}_2\text{-}N,P)_2]$ underwent a rapid chelate ring-opening reaction in DMSO. A fresh solution of **3** in $\text{DMSO-}d_6$ was monitored by NMR. The ring-opening reaction appeared complete by the time the first spectrum was acquired. The presence of a one ring-open, one ring-closed conformation was strongly suggested by the $^{31}\text{P}\{^1\text{H}\}$ NMR spectrum. Two doublets were present, one at δ 60.7 and the other at δ 45.7. The $J(\text{P-P})$ coupling constant of 24.6 Hz is indicative of two *cis* phosphorus nuclei [23]. The signal at δ 60.7 corresponds to the expected value for a chelated aminophosphine ligand bound through both P and N [11,24]. If ring-

opening of a chelated ligand occurs (Ru–N bond breaks), the ^{31}P signal for the phosphorus of that ligand would be expected to shift to higher field. This was observed for *trans*, *cis*-[RuCl₂(DMAP)] [11] and also the chemical shift is similar to that observed for the ring-opened Pt(II) complexes of aminophosphine ligands coordinated via P only [5,6]. This phenomenon has also been observed for the complex [Cp*₂Ru(DMAP)Cl] [31], for which the ^{31}P chemical shift of the ring-closed form of the complex is δ 60.9 and the ring-opened form appears at higher field at δ 38.9. After 1 week it was noted that a third signal had appeared in the ^{31}P spectrum of **3** at δ 51.4. This was a singlet, indicating equivalent phosphorus nuclei in the complex. However, even after 2 months this species never became dominant and a definite assignment was not possible. This peak may arise from a Ru-complex with 2 equiv. ring-opened ligands. No free ligand was detected and therefore, complexes with only one ligand, due to loss of a DHAP can be ruled out. The spectrum in CD₃CN is very similar. Thus **3** reacts with DMSO and CH₃CN to give a complex with one chelated aminophosphine ligand and one pendant ligand coordinated only through phosphorus. The ^1H NMR spectrum showed a variety of peaks due to the 2 inequiv. ligands, and from COSY, TOCSY and [^{31}P - ^1H] HSQC experiments it was possible to distinguish between the pendant and chelated ligands. The [^{31}P - ^1H] HSQC spectrum is shown in Fig. 2 and the COSY assignments are given in Table 2. The combined COSY and HSQC spectra allowed assignments of the ring-opened and ring-closed aminophosphine complexes to be made, and the TOCSY experiment allowed the N–H protons to be assigned. The ligand coordinated at the vacated site after ring-opening, is believed to be DMSO, the solvent used for the NMR experiments.

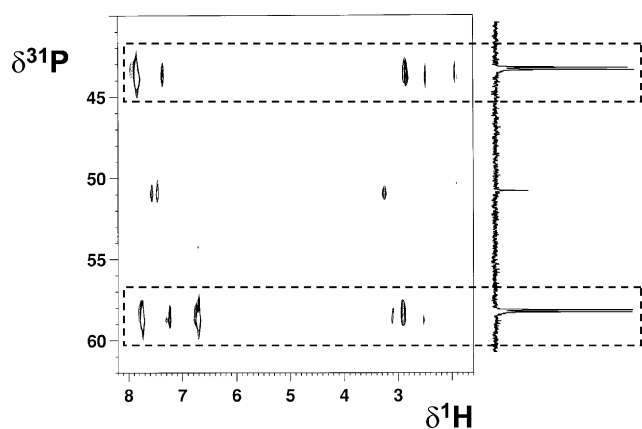


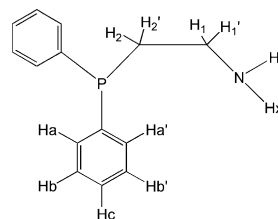
Fig. 2. [^1H , ^{31}P] 2D HSQC NMR spectrum of complex **3** after standing for 1 week in d_6 -DMSO. The dotted boxes contain peaks for the major species, the mono chelate ring-opened complex: ^{31}P doublet for ring-opened ligand at low field, and for the ring-closed ligand at high field. ^1H , ^1H 2D COSY was used to confirm the assignments (see Table 2).

Table 1
Selected bond lengths (Å) and angles (°) for complex **1**, **3**, **4** and **5**

	1	3	4	5
<i>Bond lengths</i>				
Ru–P(1)	2.247(4)	2.2552(6)		2.3122(11)
Ru–P(2)	2.252(4)	2.2565(6)		
Ru–N(1)	2.212(11)	2.1642(19)	2.20(2)	2.212(3)
Ru–N(2)	2.230(10)	2.1796(18)		
Ru–Cl(1)	2.401(4)	2.4053(6)	2.400(7)	2.3986(11)
Ru–Cl(2)	2.410(4)	2.4192(6)	2.401(7)	
Ru–O			2.18(2)	
Ru–S(1)			2.200(7)	
Ru–S(2)			2.250(5)	
<i>Bond angles</i>				
P(1)–Ru–P(2)	101.48(14)	102.80(2)		
N(1)–Ru–N(2)	93.1(4)	90.73(7)		
Cl(1)–Ru–Cl(2)	166.98(11)	164.29(2)	170.6(2)	
P(1)–Ru–N(2)	82.5(3)	82.99(5)		81.68(9)
P(2)–Ru–N(2)	83.0(3)	83.51(5)		
N(1)–Ru–O(1)			94.4(6)	

Table 2

^1H NMR chemical shifts (δ) for the chelated and pendant (ring-opened) ligands of complex **3** in DMSO- d_6



	δ (chelated ligand)	δ (pendant ligand)
N–H _x	4.97	4.23
N–H _y	4.71	4.23
H ₁	3.13	2.89
H ₁ '	2.57	1.86
H ₂	3.07	2.57
H ₂ '	2.95	1.97
H _a , H _a '	7.78 (7.36) ^a	7.89
H _b , H _b '	7.4 ^b (7.27)	7.4 ^b
H _c	7.4 ^b (6.75)	7.4 ^b

^a Figures in brackets refer to the second phenyl group.

^b Overlapped.

3.4. Cyclic voltammetry of complex **3** in CH₃CN

The Ru(III)/(II) reduction potential of ruthenium complexes may play an important role in their biological activity. It has been hypothesised that Ru(III) complexes may be prodrugs that are activated in vivo by reduction to Ru(II) [25]. Therefore, we investigated the electrochemistry of complex **3**. Acetonitrile was used to provide good solubility and allow ease of handling at various temperatures. With CH₃CN as solvent, a reversible

oxidation at 0.82 V (vs. Ag/AgCl) was observed at 298 K. The oxidised species appeared to be unstable and no peak was detected using a slow sweep rate. When the sample was cooled to 227 K, this couple was more readily observed. The redox process can tentatively be assigned to the metal centred Ru(II)–Ru(III) couple. The value of 0.82 V is much higher than the corresponding value for $[\text{RuCl}_2(\text{DMAP})_2]$ [11] which was observed at 0.326 V, and is likely to be too high to be of biological relevance.

3.5. UV–Vis spectroscopy of complex 5

The UV–Vis spectrum of **5** in DMSO changed with time (Fig. 3). The band at 326 nm gradually decreased in intensity and that at 300 nm increased concomitantly, with an isosbestic point at 320 nm. By following the absorbance decrease at 326 nm with time, assuming a first order reaction, and treating the data by the Guggenheim method [26], a first order rate-constant of $2.03 \times 10^{-4} \text{ s}^{-1}$ was obtained. This reaction can be attributed to substitution of a chloride ligand by DMSO and was inhibited in the presence of 100 mM LiCl.

3.6. Crystallography

The X-ray crystal structures of **1**, **3**, **4** and **5** are shown in Figs. 4–7. Data collection and refinement parameters are summarised in Section 2. Bond distances and angles are listed in Table 1.

The Ru(II) centres in these complexes have distorted octahedral geometries. In complex **1** the two Cl ligands are *trans* and the two chelated P–N ligands are in *cis* positions (Fig. 4). This arrangement appears to be sterically crowded, but is apparently preferred to that in which the two P atoms are *trans* because of their strong *trans* effects [27]. This is in agreement with the previously reported structure of *trans, cis*- $[\text{RuCl}_2(\text{DMAP})_2]$ [11]. There are no strong intermolecular interactions involved in the crystal packing. The Ru–P (2.247(4) and 2.252(4) Å) and Ru–Cl (2.401(4) and 2.410(4) Å) bond lengths are within the range of values typical for Ru(II) complexes [11,28]. In *trans, cis*- $[\text{RuCl}_2(\text{DMAP})_2]$ [11] it was found that the Ru–N

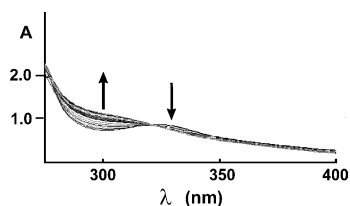


Fig. 3. The electronic absorption spectrum of complex **5** in DMSO at 298 K recorded every hour for 12 h. A pseudo first order kinetic plot using the absorbance change 326 nm gave a rate constant of $2.03 \times 10^{-4} \text{ s}^{-1}$.

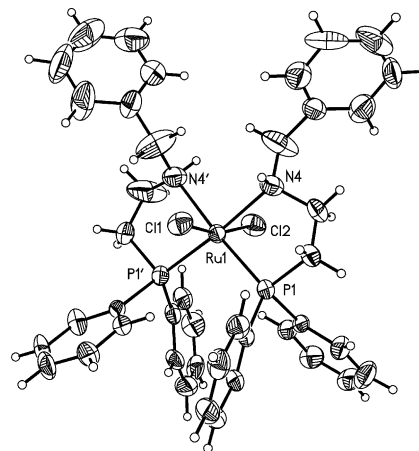


Fig. 4. X-ray crystal structure of complex **1**. Probability surfaces enclose 50% ellipsoids. The minor disorder component has been omitted.

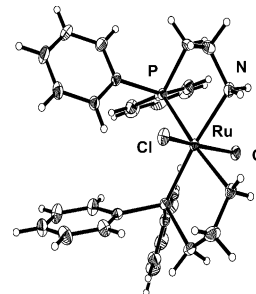


Fig. 5. X-ray crystal structure of complex **3**.

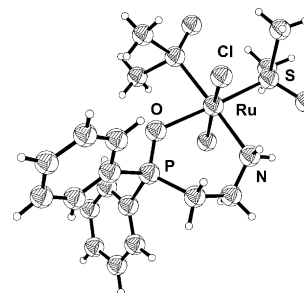


Fig. 6. X-ray crystal structure of complex **4**.

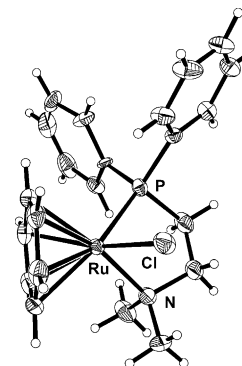


Fig. 7. X-ray crystal structure of complex **5**. The PF_6 anion is not shown.

bond lengths (mean = 2.391 Å) were considerably longer (0.2 Å) than values for P–N chelated Ru(II) complexes previously reported, for example, N *trans* to P in complexes such as *trans*-dichloro-bis(diphenylphosphino)pyridineruthenium(II) (2.13 and 2.06 Å) [29], *trans*-dichloro-*N,N*-bis-*[o*-(diphenylphosphino)benzylidene]-(ethylenediamine)ruthenium(II) (2.17 and 2.16 Å) [9], and dichlorotetra(1-(diphenylphosphino)-2-(2-pyridyl)-ethane)diruthenium(II) (2.152 and 2.157 Å) [30]. However, this effect is not seen for complex **1**, despite the similar geometry and despite having the potentially more bulky benzyl group on the nitrogens. It is possible that the presence of H as the second substituent on N reduces the steric effects. The benzyl groups point away from each other, thereby greatly reducing the steric hindrance. The crystal structures of Pd(II) and Pt(II) complexes with the same ligand (DPEBA) do not contain any metal–N bonds probably because the benzyl groups are too sterically demanding and prevent chelation in these square-planar structures [5]. The bending of the Cl–Ru–Cl axis (166.98(11)°) probably results from crowding caused by the phenyl substituents on phosphorus and is greater than was found for [RuCl₂(DMAP)₂] (172°) [11]. Cl–Ru–Cl bond angles as low as 165.4° have been reported in the literature, e.g. for *trans*-dichloro-*N,N*-bis-*[o*-(diphenylphosphino)benzylidene]-(ethylenediamine)ruthenium(II) [9].

The structure of complex **3** is shown in Fig. 5. The two chloride ligands are *trans* and the aminophosphine ligands are *cis*. The lack of steric hindrance from the N–H groups is apparent from the Ru–N bond lengths of 2.1642(19) and 2.1796(18) Å which are the shortest Ru–N bond lengths of the complexes **1**, **4**, **5**, [RuCl₂(DMAP)₂], [11] and [Cp*Ru(DMAP)Cl] [31]. The hydrogens allow the nitrogens to move closer to the metal as compared with bulkier substituents such as methyl or benzyl groups. The bite angle of the chelate rings is approximately 83°, smaller than for the other complexes. The closer approach of the N atoms in **3** compared with the other bis-aminophosphine complexes discussed here can be seen from the N–Ru–N angle of 90.73(7)°, compared with 93.1(4)° for **1** and 94.6(3)° for *trans*, *cis*-[RuCl₂(DMAP)₂] [11]. The Ru–Cl bond lengths (2.4053(6) and 2.4192(6) Å) are typical for octahedral Ru(II) complexes. The Cl–Ru–Cl bond angle of 164.29(2)° is very low, highly distorted from linearity. The phenyl rings of adjacent PPh₂ groups are almost perpendicular, allowing them to pack closely together.

In complex **4** (Fig. 6), the aminophosphine oxide ligand forms a six-membered chelate ring, binding to Ru through O and N in *cis* equatorial positions. The two chloride ligands are *trans* in the axial positions and the two DMSO ligands fill the other two equatorial sites. Both DMSO molecules are coordinated through sulfur, and one is *trans* to N and the other is *trans* to O. Sulfur is a mildly π -accepting ligand, and it is reasonable to

expect two π -accepting ligands to be located orthogonal to each other [32]. The Ru–O bond length is 2.18(2) Å, similar to those in the chelated phosphine-oxide complex *trans*-[RuCl₂{*o*-C₆H₄(PMePh)₂}{*o*-C₆H₄(PMePh)-P(O)MePh}] which has a Ru–O bond length of 2.166(5) Å [33], the arene complex [(η^6 -*p*-cymene)RuCl(η^2 -Ph₂PCH₂P(O)Ph₂)] [SbF₆] (Ru–O = 2.154(3) Å), [34] and the mixed-valence Ru(II/III) binuclear compound [Ru₂(μ -O₂CC₄H₃S)₄(OPPh₃)₂]⁺ (Ru–O(P) = 2.216(7) Å [35]).

The Ru–S bonds for the two DMSO ligands of complex **4** are significantly different from each other, the longest is Ru–S *trans* to N (2.250(5) Å). The Ru–S bond *trans* to oxygen, however, is quite short, 2.200(7) Å, similar to that for [Ru(DMSO)(NH₃)₅]²⁺, 2.188(3) Å [36]. The shortness of the Ru–S bond in the latter amine complex has been attributed [36] to an M⁺ = S–O[–] component, a conclusion supported by the relatively long S–O bond length of 1.527(7) Å. For uncoordinated sulfoxides, the average S–O bond distance is 1.4918(9) Å. This value is lengthened to 1.528(1) Å upon oxygen coordination to metal ions, while it is reduced to 1.4731(6) Å upon sulfur coordination [37]. Complex **4**, has a typical S–O bond length (1.48(2) Å), a feature found in S-bound DMSO complexes such as [Ru(II)Cl₃(DMSO)₃][–] (mean 1.48 Å) [38] and [Ru(DMSO)₆]²⁺ (mean 1.482 Å) [39]. Both Ru–S bonds in complex **4** are shorter than those in *cis*-[RuCl₂(DMSO)₄] (mean 2.267 Å), its isomer *trans*-[RuCl₂(DMSO)₄] (mean 2.352 Å) [12], and [Ru(DMSO)₆]²⁺ (mean 2.259 Å). The Cl–Ru–Cl angle of 170.6(2)° is again distorted from linearity. The Ru–N bond length (2.20(2) Å) is in the expected range [9,29,30].

[(η^6 -C₆H₆)Ru(Me₂NCH₂CH₂PPh₂-*N,P*)Cl][PF₆] (**5**) (Fig. 7) has a piano-stool type geometry typical of Ru(II) arene complexes, with an η^6 -arene ring forming the seat and the three ligands forming the legs of the stool. The Ru–P bond length in **5** (2.3122(11) Å) is similar to those of [Cp*Ru(DMAP)Cl] (2.289(1) Å [31]). However the Ru–N bond length for **5**, 2.212(3) Å, is significantly shorter than the value of 2.260(2) Å for the Cp* complex, but longer than the values of 2.11–2.13 Å found for [(η^6 -arene)Ru(en)Cl][PF₆] where arene is benzene or a substituted benzene, and en is ethylenediamine [40]. The Ru–Cl bond (2.3986(11) Å) is shorter than for [Cp*Ru(DMAP)Cl] (2.441(1) Å), but within the range for Ru–Cl bonds of half-sandwich complexes of Ru(II) [40,41]. The P–Ru–N angle of 81.68(9)° is close to those found for [Cp*Ru(DMAP)Cl] and [(η^6 -C₆H₆)Ru(en)Cl][PF₆] [31,40].

4. Conclusions

We have previously reported that square-planar Pt(II) aminophosphine complexes can exist in ring-closed

(chelated) and ring-opened (with the pendant arm coordinated through phosphorus only) forms in aqueous solution, and that the extent of ring opening can be controlled by the substituents on N, the size of the chelate ring, the pH and chloride concentration [5,6,42]. Some of these complexes were also cytotoxic to cancer cells. In this work we have investigated the structures and solution properties of Ru(II) analogues, since there is also significant current interest in the anticancer activity of ruthenium complexes [25].

The X-ray crystal structures of the Ru(II) aminophosphine complexes *trans, cis*-[RuCl₂(H(Bz)NCH₂-CH₂PPh₂-*N,P*)₂] (**1**) and *trans, cis*-[RuCl₂(H₂NCH₂-CH₂PPh₂-*N,P*)₂] (**3**) showed that analogues of the Pt(II) complexes can be prepared, but now as octahedral complexes containing additional axial chloride ligands as expected for Ru(II). Steric crowding causes a marked distortion of the Cl–Ru–Cl axis from linearity. Complex **3** underwent facile chelate ring-opening in DMSO and CH₃CN solutions which might be promising for anticancer activity involving attack on DNA bases. However, in general we obtained only low yields of these complexes and, unlike the Pt(II) species which are charged, the aqueous solubility of the neutral Ru(II) complexes was very low. This problem will need to be addressed if the biological properties of these complexes are to be further explored.

The aminophosphine complex [(η⁶-C₆H₆)Ru(Me₂N-CH₂CH₂PPh₂-*N,P*)Cl][PF₆] (**5**) is an analogue of active ethylenediamine complexes which bind strongly to DNA [40], and complexes in this arene Ru(II) series may be useful anticancer agents.

5. Supplementary material

CCDC deposition numbers: complex **1**, 178906; complex **3**, 178903, complex **4** 178905; complex **5**, 178904. Copies of this information may be obtained free of charge from The Director, CCDC, 12 Union Road, Cambridge, CB2 1EZ, UK (fax: +44-1223-336-033; e-mail: deposit@ccdc.cam.ac.uk or <http://www.ccdc.cam.ac.uk>).

Acknowledgements

We thank the EPSRC, BBSRC, Wolfson Foundation and Royal Society for their support for this work, Dr. Lesley Yellowlees for assistance with electrochemistry, Dr. John Parkinson with NMR spectroscopy, members of EC COST D8 and D20 for stimulating discussions, CCLRC and Dr. Simon Teat (Daresbury Laboratory) for Synchrotron beam time, and Johnson Matthey for the loan of some of the ruthenium.

References

- [1] (a) M. Basset, D.L. Davies, J. Neild, L.J.S. Prouse, D.R. Russell, *Polyhedron* 10 (1991) 501; (b) K. von Issleib, A. Kipke, V. Hanfeld, *Z. Anorg. Allg. Chem.* 444 (1978) 5; (c) K. von Issleib, A. Kipke, *Z. Anorg. Allg. Chem.* 464 (1980) 176; (d) G.K. Anderson, R. Kumar, *Inorg. Chem.* 23 (1984) 4064; (e) M.M.T. Khan, E.R. Rao, *Polyhedron* 6 (1987) 1727; (f) M.M.T. Khan, V.V.S. Reddy, H.C. Bajaj, *Inorg. Chim. Acta* 130 (1987) 163; (g) V.V.S. Reddy, S. Vijay, *J. Mol. Catal.* 45 (1988) 73.
- [2] S. Chatterjee, D.C.R. Hockless, G. Salem, P. Waring, *J. Chem. Soc., Dalton Trans.* (1997) 3889.
- [3] J. Reedijk, *J. Chem. Soc., Chem. Commun.* (1996) 801.
- [4] S.J. Berners-Price, R.J. Bowen, M.J. McKeage, P. Galettis, L. Ding, B.C. Baguley, W. Brouwer, *J. Inorg. Biochem.* 67 (1997) 154.
- [5] A. Habtemariam, B. Watchman, B.S. Potter, R. Palmer, S. Parsons, A. Parkin, P.J. Sadler, *J. Chem. Soc., Dalton Trans.* (2001) 1306.
- [6] A. Habtemariam, P.J. Sadler, *J. Chem. Soc., Chem. Commun.* (1996) 1785.
- [7] C. Muddalige, S.J. Rettig, W.R. Cullen, R.B. James, *J. Chem. Soc., Chem. Commun.* (1993) 830.
- [8] M.M.T. Khan, A.P. Reddy, *Polyhedron* 6 (1987) 2009.
- [9] J.-X. Gao, H.-L. Wan, W.-K. Wong, M.-C. Tse, W.-T. Wong, *Polyhedron* 15 (1996) 1241.
- [10] L. Costella, A. del Zotta, A. Mezzetti, E. Zangrando, P. Rigo, *J. Chem. Soc., Dalton Trans.* (1993) 3001.
- [11] Z. Guo, A. Habtemariam, P.J. Sadler, B.R. James, *Inorg. Chim. Acta* 273 (1998) 1.
- [12] E. Alessio, G. Mestroni, G. Nardin, W.M. Attia, M. Calligaris, G. Sava, S. Zorzet, *Inorg. Chem.* 27 (1988) 4099.
- [13] E.W. Abel, *J. Chem. Soc.* (1959) 3178.
- [14] F.B. McCormick, D.D. Cox, W.B. Gleason, *Organometallics* 12 (1993) 610.
- [15] P.T. Beurskens, G. Beurskens, W.P. Bosman, R. de Gelder, S. Garcia-Granda, R.O. Gould, R. Israel, J.M.M. Smits, *Crystallography Laboratory, University of Nijmegen, Nijmegen, The Netherlands*, 1996.
- [16] G.M. Sheldrick, *SHELXTL*, version 5, Bruker Analytical X Ray, Madison, WI, 1995.
- [17] G.M. Sheldrick, *SADABS: Area-Detector Absorption Correction*, Siemens Industrial Automation, Madison, WI, 1996.
- [18] D. Cromer, R. von Dreele, in: L.J. Farrugia (Ed.), *FPRIME* Incorporated in the WINGX Suite of Programs, *J. Appl. Crystallogr.* 32 (1999) 837.
- [19] (a) E.B. Boyer, P.A. Harding, S.D. Robinson, *J. Chem. Soc., Dalton Trans.* (1986) 1771; (b) G. Sia, A.L. Rheingold, B.J. Haggerty, D.W. Meek, *Inorg. Chem.* 31 (1992) 900; (c) A. Albinati, Q. Jiang, H. Ruegger, L.M. Venanzi, *Inorg. Chem.* 32 (1993) 4940.
- [20] J.Y. Shen, C. Slugovc, P. Wiede, K. Mereiter, R. Schmid, K. Kirchner, *Inorg. Chim. Acta* 268 (1998) 69.
- [21] A. Dovletoglou, S.A. Adeyemi, M.H. Lynn, D.J. Hodgson, T.J. Meyer, *J. Am. Chem. Soc.* 112 (1990) 8989.
- [22] B.A. Mayer, B.K. Sipe, T.J. Mayer, *Inorg. Chem.* 20 (1981) 1475.
- [23] (a) M.M. Taqui-Khan, V. Vijay, V.V.S. Reddy, *Inorg. Chem.* 25 (1986) 208; (b) J.C. Briggs, C.A. McAuliffe, G. Dyer, *J. Chem. Soc., Dalton Trans.* (1984) 423; (c) D.F. Gill, B.E. Mann, B.L. Shaw, *J. Chem. Soc., Dalton*

- Trans. (1973) 311;
(d) G.K. Anderson, R. Turner, *Inorg. Chem.* 24 (1984) 4064.
- [24] P.E. Garrou, *Chem. Rev.* 81 (1981) 229.
- [25] M.J. Clarke, F. Zhu, D.R. Frasca, *Chem. Rev.* 99 (1999) 2511.
- [26] D.P. Shoemaker, C.W. Garland, *Experiments in Physical Chemistry*, McGraw-Hill, New York, 1962, p. 222.
- [27] F.A. Cotton, G. Wilkinson, *Advanced Inorganic Chemistry*, 4th ed., Wiley, New York, 1980, p. 1200.
- [28] (a) A.G. Orpen, L. Brammer, F.H. Allen, O. Kennard, D.G. Watson, R. Taylor, *J. Chem. Soc., Dalton Trans.* (1989) 83;
(b) A.M. Joshi, I.S. Thorburn, S.J. Rettig, B.R. James, *Inorg. Chim. Acta* 283 (1992) 198.
- [29] D. Drommi, F. Nicolo, C.G. Arena, G. Bruno, F. Faraone, R. Gobetto, *Inorg. Chim. Acta* 221 (1994) 109.
- [30] L. Costella, A. Del Zotto, A. Mezzetti, E. Zangrando, P. Rigo, *J. Chem. Soc., Dalton Trans.* (1993) 3001.
- [31] K. Mauthner, C. Slugovc, K. Mereiter, R. Schmid, K. Kirchner, *Organometallics* 16 (1997) 1956.
- [32] M.M. Olmstead, Y. Maisonnat, J.P. Farr, A.L. Balch, *Inorg. Chem.* (1981) 4061.
- [33] S.R. Hall, B.W. Shelton, A.H. White, *Aust. J. Chem.* 36 (1983) 267.
- [34] J.W. Faller, P.B. Patel, M.A. Albrizzio, M. Curtis, *Organometallics* 18 (1999) 3096.
- [35] M.C. Barral, R. Jiménez, J.L. Priego, E.C. Royer, M.J. Saucedo, F.A. Urbanos, *Polyhedron* 14 (1995) 2419.
- [36] F.C. March, G. Ferguson, *Can. J. Chem.* 49 (1971) 3590.
- [37] (a) M. Calligaris, *Croat. Chem. Acta* 72 (1999) 147;
(b) M. Calligaris, O. Carugo, *Coord. Chem. Rev.* 153 (1996) 83.
- [38] R.S. McMillan, A. Mercer, B.R. James, J. Trotter, *J. Chem. Soc., Dalton Trans.* (1995) 1006.
- [39] A.R. Davies, F.W.B. Einstein, N.P. Farrell, B.R. James, R.S. McMillan, *Inorg. Chem.* 17 (1978) 1965.
- [40] R.E. Morris, R.E. Aird, P. del S. Murdoch, H. Chen, J. Cummings, N.D. Hughes, S. Parsons, A. Parkin, G. Boyd, D.I. Jodrell, P.J. Sadler, *J. Med. Chem.* 44 (2001) 3616.
- [41] I. los de Rios, M.J. Tenorio, J. Padilla, M.L. Puerta, P. Valerga, *J. Chem. Soc., Dalton Trans.* (1996) 377.
- [42] A. Habtemariam, J.A. Parkinson, N. Margiotta, T.W. Hambley, S. Parsons, P.J. Sadler, *J. Chem. Soc., Dalton Trans.* (2001) 362.